

## Optimization of chromium (VI) adsorption by novel nano-pumice modified by cationic surfactant from aqueous media using the response surface method: isotherm and kinetic studies

Fatemeh Eslami<sup>a</sup>, Ramin Nabizadeh Nodehi<sup>a</sup>, Simin Nasser<sup>a</sup>, Mehdi Salari<sup>b</sup>, Amir Hossein Mahvi<sup>a,c,\*</sup>, Faramarz Doulati Ardejani<sup>d,\*</sup>

<sup>a</sup>Department of Environmental Health Engineering, School of Public Health, Tehran University of Medical Sciences, Tehran, Iran, Tel. 00982188954914; emails: [ahmahvi@yahoo.com](mailto:ahmahvi@yahoo.com) (A.M. Mahvi), [fatemeh.eslami6397327@gmail.com](mailto:fatemeh.eslami6397327@gmail.com) (F. Eslami), [rnabizadeh@tums.ac.ir](mailto:rnabizadeh@tums.ac.ir) (R.N. Nodehi), [naserise@tums.ac.ir](mailto:naserise@tums.ac.ir) (S. Nasser)

<sup>b</sup>Ph.D student of Environmental Health Engineering, School of Public health, Hamadan University of Medical Sciences, Hamadan, Iran, email: [msalari\\_22@yahoo.com](mailto:msalari_22@yahoo.com)

<sup>c</sup>Center for Solid Waste Research, Institute for Environmental Research, Tehran University of Medical Sciences, Tehran, Iran

<sup>d</sup>School of Mining, College of Engineering, University of Tehran, Iran, Tel. 00982182084249; email: [fdoulati@ut.ac.ir](mailto:fdoulati@ut.ac.ir)

Received 20 April 2019; Accepted 18 September 2019

### ABSTRACT

The present study focused on the evaluation of modified nano-pumice with hexadecyl trimethyl ammonium bromide (HDTM.Br) surfactant in adsorption of Cr(VI) from aqueous environments. The effects of pH (3–9), contact time (30–120 min), Cr(VI) concentration (0.05–1 mg/L) and adsorbent dose (0.1–1 g) on the adsorption rate were designed, modeled and optimized according to central composite design-response surface methodology (CCD-RSM). Considering ANOVA and regression analyses, the adsorption process better follows the quadratic polynomial model with  $p$ -value < 0.005,  $R^2 = 0.9906$ . The model adequacy established based on CCD-RSM is quite clear with regard to the value of lack of fit test, which is 0.75. The optimum conditions were obtained at pH 3, Cr(VI) concentration 0.05 mg/L, adsorbent dose 1 g/L and contact time 120 min, respectively. The maximum adsorption capacity of Cr(VI) was found to be 0.24 mg/g. Kinetic and isotherm studies showed that the adsorption process is better described with pseudo-second kinetics with  $R^2 = 0.9983$  and Freundlich isotherm with  $R^2 = 0.9971$ . Given to the highest efficiency of Cr(VI) adsorption (about 96%) by pumice/HDTM.Br nano composite, the composite can be proposed as a promising adsorbent for the removal of Cr(VI) in water under specific conditions.

**Keywords:** Chromium (VI) adsorption; Modified nano-pumice; Cationic surfactant; Response surface methodology; Aqueous environments

### 1. Introduction

Chromium (VI) is a very toxic element that has carcinogenic, mutagenic, and teratogenic properties for living organisms [1]. Cr(VI) basically exists in the forms of chromium and dichromate anions in aqueous systems [2]. These compounds often are introduced into the aqueous environments through

discharging wastewater of various industrial processes and operations, such as metal smelting, leather tanning, cement protection, paint, textile and steel industries [3]. The maximum concentration of Cr(VI) in surface water and drinking water should be in the range of safe concentrations presented by health authorities and if its concentration in drinking water exceeds safe level, it may cause health disorders such as vomiting, skin irritation, lung cancer, kidney hemorrhage and damage to the liver and stomach. Several conventional

\* Corresponding authors.

techniques such as precipitation, electrochemical, electro-coagulation, ion exchange, reverse osmosis and adsorption were reported for the removal of heavy metals from aqueous environments [4–7]. The adsorption process is widely used in water and wastewater treatment operations due to some merits such as low cost, simple design and operation, and the ability to remove contaminants at low concentrations [8]. So far, numerous adsorbents, such as activated carbon, fly ash, organic polymers, oxidants and natural adsorbents such as zeolite, kaolinite, alumina, wheat bran, corn bran, sawdust, hazelnut ash, chitosan, pumice and other cost-effective adsorbents, have been investigated in their abilities to adsorb chromium (VI) [9].

Economic issues and the need to revive the adsorbents have led researchers to study and find cheap and affordable adsorbents. In recent decades, geometric materials have shown to be extensively used in water and wastewater treatment processes because of both good adsorption and cheap prices [10].

Pumice stone is one of the most widely used geometric compositions in the field of removing contaminants from aqueous systems. This stone has been characterized by high porosity, light weight and large specific surface area (SSA), with respect to that most of its structure consists of  $\text{SiO}_2$  [11]. Application of modified natural adsorbents for adsorption of various organic and inorganic anions from aqueous solutions has been investigated. Cationic surfactants are used to modify the external surfaces of different materials and increase their ion exchange capacity because these compounds tend to be negatively exchanged [12]. Nanotechnology is the engineering of functional systems at the molecular scale, offering new products and process alternatives for water purification. The advantage of these materials is to have a large surface to volume ratio. Various studies have been carried out to investigate pumice and nano-pumice capability to remove compounds from aqueous solutions such as cadmium [13], atrazine [14], chromium [15], arsenic [16], fluoride [17] and color [18], during adsorption and catalytic processes.

On the basis of these facts, the major objective of this study was to design, model and optimize experiment conditions using CC-RSM approach, in Cr(VI) adsorption with modified nano pumice with hexadecyl trimethyl ammonium bromide (HDTM.Br) surfactant (nano pumice/HDTM.Br composite). The independent variables evaluated during the study included pH, contact time, initial concentration of Cr(VI) and adsorbent dose. Finally, isotherm and kinetic studies were carried out for the adsorption process.

## 2. Materials and methods

### 2.1. Preparation of adsorbent

#### 2.1.1. Nano-pumice preparation

The pumice stone used in this study was supplied from Tekmeh Dash region, East Azerbaijan, Iran. First, pumice was crushed using a cone crusher up to  $\leq 3$  cm dimensions, and then these dimensions was reduced to 100  $\mu\text{m}$  using a micronizer (Siebtechnik Co., France). Finally, the obtained particles from this stage were converted to a nanometer size by a satellite mill (FRITSCH EQ-PC1-12, Germany). To remove the primary impurities, the sample obtained from

the previous step was washed several times with distilled water. In order to increase the porosity of the adsorbent, the nano-pumice was added into 0.1 N chloride acid solution (37%) for 48 h at room temperature. Afterwards, the adsorbent was washed with double-distilled water several times until the outlet turbidity reaching less than 1 NTU and pH to 7. The sample was then dried in a laboratory oven at 105°C for 8 h.

#### 2.2.2. Preparation of pumice/HDTM.Br nano composite

In order to modify the adsorbent, 20 g of the nano-pumice prepared in the previous step, was added in 2 L of HDTM.Br solution (2.5 mmol/L), and the solution pH was adjusted to 10. The resulting solution was stirred at 220 rpm at room temperature for 10 h and then separated by a Whatman filter paper. The resulting mixture was dried at 120°C for 2.5 h, and then washed using double-distilled water. Again, it was dried at 120°C for 6 h. The modified pumice/HDTM.Br nano composite was prepared and used in the other stages of the study.

#### 2.2. Determination of physicochemical properties of nano pumice/HDTM.Br composite

SSA pore diameter and volume of nano-pumice adsorbent were determined before and after modification by Brunauer–Emmett–Teller (BET) (nitrogen sorption isotherm) method (Belsorp mini II, Bel model, Japan). The physicochemical and crystalline properties of pumice/HDTM.Br nano composite were also studied by X-ray fluorescence analysis (XRF) and X-ray diffraction (XRD) (Xpert Philips PW 3040/60, Lum Cu, The Netherlands), respectively. The pre- and post-modification morphology and surface properties of nano-pumice were evaluated by FE-SEM analysis (Field Emission Scanning Electron Microscopy, S4160 manufactured by HITACHI Co., Japan). To measure the particle size of pumice/HDTM.Br nano composite, the atomic force microscope (AFM) (Model DS-95-50E) was used. The Fourier transform infrared (FTIR) analysis (PerkinElmer spectrophotometer device, model Nicolet.760, USA) was carried out based on electromagnetic radiation adsorption and vibrational mutation analysis of molecules and multi-atom ions in nano-pumice adsorbent before and after modification. Finally,  $\text{pH}_{\text{zpc}}$  (adsorbent's point of zero charge [pzc]) was determined for pumice/HDTM.Br nano composite to determine the surface charge.

#### 2.3. RSM-based experiment design

In the present study, to evaluate the linear, quadratic and interactive effects of independent variables on the response Cr(VI) removal efficiency, as well as to make optimization of experiment conditions and statistical analyses, CCD-RSM method was used (R software). Affective variables on Cr(VI) adsorption were selected based on other studies carried out in this field. Accordingly, the effect of four factors, namely pH, contact time, initial concentration and adsorbent dose has been investigated in five levels, the maximum, minimum and mean values of which are presented in Table 1. The number of experiments was calculated according to the following

Table 1  
Maximum, minimum and average values of each independent variables in experiments

Variablez	Symbol	Max	Min	AVG
pH	$X_1$	9	3	6
Contact time (min)	$X_2$	120	30	75
Initial concentration of Cr(VI) (mg/L)	$X_3$	1	0.05	0.53
Absorbent dose (g/L)	$X_4$	1	0.1	0.55

equation, where  $k$  is the number of variables and  $C$  represents the number of repetitions.

$$N = 2k + 2k + C \quad (1)$$

Finally, a total of 30 experimental tests were obtained as given in Table 1.

The effect of the independent studied variables on the response rate ( $Y$ ) was determined based on the quadratic model, which is presented in Eq (2):

$$Y = a_0 + \sum a_i x_i + \sum a_{ii} x_i^2 + \sum a_{ij} x_i x_j \quad (2)$$

where  $Y$  value indicates the predicted adsorption,  $a_0$  is the y-intercept,  $a_i$  is the line gradient of the  $x_i$  factor ( $i = 1, 2, 3, 4$ ),  $a_{ii}$  is the regression coefficient of quadratic effect of  $x_i$  and  $a_{ij}$  donates the regression coefficient of the combined effect of  $x_i$  and  $x_j$  variables.

#### 2.4. Batch experiments

All experiments were carried out in a 200-mL batch reactor in a laboratory scale. In order to make the desired concentrations in this study, Cr(VI) stock solution was prepared by dissolving potassium dichromate ( $K_2Cr_2O_7$ ) in 100 mL of double distilled water. As earlier stated, the variables of time, pH, contaminant concentration and adsorbent dose were examined to reveal their effects on removal efficiency as shown in Table 1. All the experiments was conducted in the in the 200-mL flasks containing 100 mL solution. The samples were kept under mixing using a reciprocating shaker at 220 rpm until the specified times. At the end of each experiment, the solution was centrifuged at 5,000 rpm for 10 min and subsequently filtered by means of Whatman 0.45  $\mu$ m filter paper to separate the solid phase from the liquid phase. In order to measure the residual concentration of Cr(VI), 25 mL volume taken from the sample was adjusted at pH  $2 \pm 2.5$  by adding concentrated phosphoric acid. Then, 0.5 mL of diphenylcarbazide was added to the solution using an automatic pipette, and 5–10 min was taken into account to create a full purple color of the solution. Finally, the amount of light adsorption at wavelength of 540 nm by the solution was measured using UV/VIS Spectrophotometer (PerkinElmer, Lambda 25). 1 N NaOH and 1 N  $H_2SO_4$  solutions were used to adjust pH solution measured by a pH meter (Metrohm E520, Switzerland). All experiments were performed in accordance of standard methods for the examination of water and wastewater [19].

In order to determine the adsorption efficiency and capacity, Eqs. (2) and (3) were used, respectively, where  $C_0$

is the initial concentration of the contaminant (mg/L),  $C_e$  is the concentration of contaminants in the equilibrium time (mg/L),  $E$  is the removal efficiency (%),  $q_e$  is the adsorption capacity (mg/g),  $V$  is the sample size (L) and  $M$  is the adsorbent mass (g):

$$q_e = \frac{V}{M} \times (C_0 - C_e) \quad (3)$$

$$Y(\%) = \frac{C_0 - C_e}{C_0} \times 100 \quad (4)$$

#### 2.5. Optimization of factors affecting adsorption rate

The optimization was carried out in the Excel software to achieve the conditions ensuring the highest Cr(VI) removal percentage. This operation is carried out using a repeatable numerical method using the Solver tool in Excel software. At the beginning of the experiment, the real coefficients of the regression model and then the minimum and maximum values of independent variables were introduced into the software. The central points of independent variables are considered as an initial guess for the variables in question. The removal efficiency can be calculated by the regression equation according to the model coefficients and the initial guess numbers. Finally, the optimal value of each of the four variables is determined by defining the removal rate in case of maximum efficiency conditions, by changing the values of the four variables as well as by considering the constraints in such way that the value of central points are less than the maximum values and above the minimum values.

#### 2.6. Adsorption isotherms and kinetics

After determining the optimal conditions of the studied variables, isotherm studies were used to study the adsorption of the contaminant into the adsorbent and maximum adsorption capacity of pumice/HDTM.Br nano composite. Isotherm studies were performed using the mathematical equations of Freundlich, Langmuir and Temkin isotherms under optimal conditions in terms of contact time, pH and adsorbent dose under different concentrations of Cr(VI). Kinetic studies were performed to determine the rate and type of adsorption using pseudo-first-order, pseudo-second-order and intraparticle diffusion in optimal conditions in terms of Cr(VI) concentration, adsorbent dose, pH and different contact times.

### 3. Results and discussion

#### 3.1. Nano-pumice analysis

##### 3.1.1. X-ray fluorescence analysis

The purpose of XRF is to carry out an elemental analysis and determine the percentage of compounds in the adsorbent, and XRD analysis (XRD) is carried out to identify the crystalline phases in the adsorbent, both of which are carried out using X-ray characteristics [20]. The results of XRF test shown in Table 2 indicate that the highest percentages of nano-pumice structure are occupied by  $SiO_2$ ,  $Al_2O_3$ ,  $CaO$ ,  $Fe_2O_3$ ,  $K_2O$ ,

Na<sub>2</sub>O, while MgO, TiO<sub>2</sub>, Cl<sub>2</sub>O<sup>-</sup>, P<sub>2</sub>O<sub>5</sub>, SO<sub>3</sub> and SrO oxides constitute lower percentages of the total adsorbent mass. Among them, SiO<sub>2</sub> and Al<sub>2</sub>O<sub>3</sub> are considered as the two major components. SiO<sub>2</sub> alone accounts for about 70.94% of the nano-pumice structure. Other studies have referred to SiO<sub>2</sub> as the main composition of the pumice structure [21]. Therefore, the remarkable presence of silicon and aluminum ions in the adsorbent is noteworthy, because of acting as adsorption sites. Also, the negative charge of the silicate layer is an effective factor in absorbing the cationic detergent, HDTM.Br, for the synthesis of pumice/HDTM.Br nano composite.

### 3.1.2. XRD analysis

The XRD pattern shows peaks scattered between the diffraction angles of 8.9° and 30°. The largest peaks were observed at diffraction angles of 21° and 24°, which belonged to SiO<sub>2</sub> and Al<sub>2</sub>O<sub>3</sub>, respectively (Fig. 1). As for the

Table 2  
Chemical components of XRF analysis of nano-pumice samples from Tekmeh Dash region

Component	Percent %
SiO <sub>2</sub>	70.94
Al <sub>2</sub> O <sub>3</sub>	6.86
CaO	6.76
Fe <sub>2</sub> O <sub>3</sub>	3.98
K <sub>2</sub> O	5.41
Na <sub>2</sub> O	0.97
MgO	0.141
TiO <sub>2</sub>	0.63
Cl <sup>-</sup>	0.35
P <sub>2</sub> O <sub>5</sub>	1.47
SO <sub>3</sub>	<0.0005

oxide compounds present in the nano-pumice, it can be predicted how it functions in the adsorption process because oxidation compounds in contact with water make hydroxyl compounds. For as much as in hydroxyl groups, silicon atoms tend to maintain their oxygen orientation. As a result, they tend to absorb ions and positive charge compounds (cationic detergents) [20]. Finally, Cr(VI) anion adsorption is performed by pumice/HDTM.Br nano composite. The amount of SiO<sub>2</sub> and Al<sub>2</sub>O<sub>3</sub> of the selected nano-pumice in this study differs from those of other studies, which can be attributed to the difference in the composition of the geological structure of the pumice source.

### 3.1.3. Field emission scanning electron microscopy

We evaluated morphology, apparent characteristics and particle size of the nano-pumice before modification (Fig. 2a) and after modification (Fig. 2b), (magnification 20 kx) using FESEM analysis. As shown in Fig. 2a, nano-pumice has a porous surface with dimensions in the nanometer range (<100 nm), which increases the SSA of this adsorbent. The large SSA will increase the level of contact between Cr and the contaminant, thus increasing the adsorption efficiency. It should be noted that the black background of this image is due to the gold coating used on these particles to better perform FESEM analysis. As shown in Fig. 2b, it can be seen that the morphology of the nano-pumice surface has changed after surfactant modification, indicating that the modification operation has been well carried out. However, the important occurrence observed during the process of adsorbent modification by cationic surfactants was the coagulation and enlargement of nano-pumice particles. This phenomenon can be explained by referring to the fact that surfactant cautions during contact with nano-pumice play an effective role in binding these particles because of the electrostatic attraction force between the nano-pumice particles (negative charge), and surfactant ions (positive charge). Not

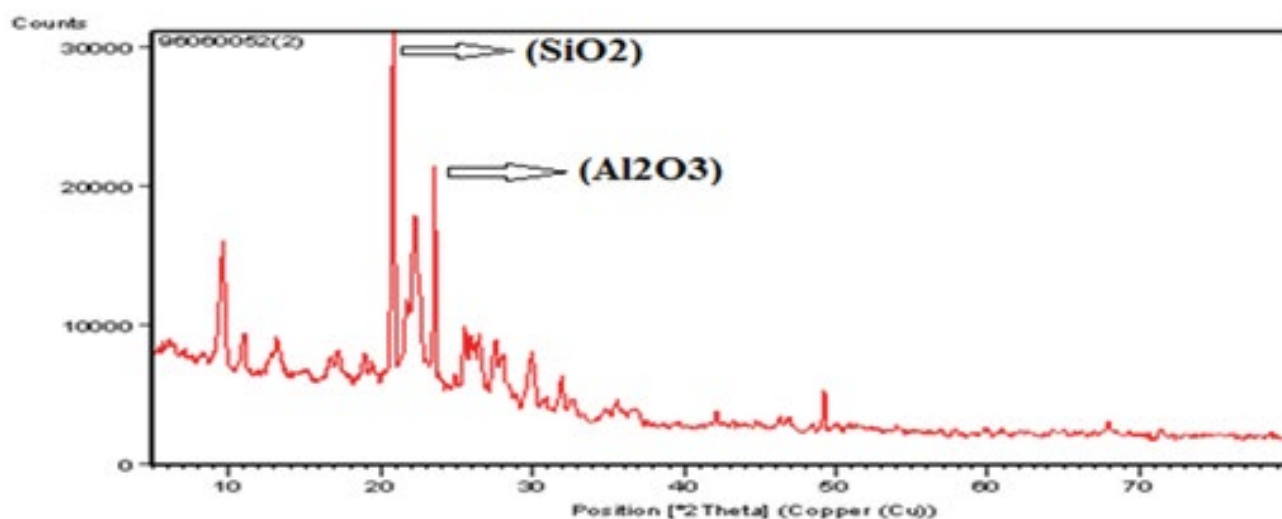


Fig. 1. XRD pattern of the nano-pumice.

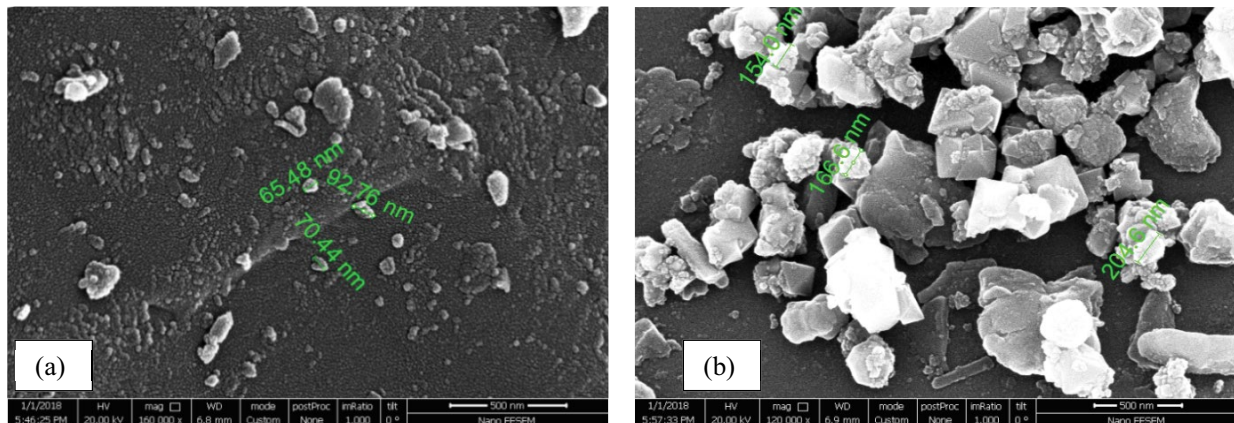


Fig. 2. FESEM images of the nano-pumice (a) and the pumice/HDTM.Br nano composite (b).

studies have shown so far these post modification changes in surface and particle size of the adsorbent.

#### 3.1.4. AFM analysis

AFM is a microscope that uses ionic force and atomic thrust to create a virtual image of the object surface and provide accurate information about the morphology and surface structure as well as the physiochemical properties of the sample considering its high sensitivity to atomic forces, such as van der Waals, bonding and electrostatic forces with high imaging precision [22]. Therefore, AFM analysis was used in this research in order to ensure the nano-adsorption structure function and to determine the size of nano-pumice particles. According to the AFM analysis images (Fig. 3), the mean particle size of the sample was determined to be between 2.62 and 98 nm, which is below 100 nm, and in accordance with the observed sizes in the FESEM analysis images. The color spectrum suggests surface morphological changes, which, in turn, show the adsorption sites on the nano-pumice surface and also the high capacity of the nano-pumice in the adsorption process. The results of the AFM and FESEM analysis showed that the particle size is less than 100 nm, which is consistent with the results of the previous study [13].

#### 3.1.5. BET analysis

Specific surface area, pore diameter and volume of the adsorbent were studied using BET analysis. The values of above parameters were 6.4693 m<sup>2</sup>/g, 26.742 nm and 4.3 cm<sup>3</sup>/s for nano-pumice, respectively, and 9.79 m<sup>2</sup>/g, 19.6 nm and 4.79 cm<sup>3</sup>/s for pumice/HDTM.Br nano composite, respectively. The results of the BET analysis indicate that the SSA of the nano-pumice increased after modification but its mean pores diameter and pore volume decreased. This post modification elevated SSA can be attributed to the removal of impurities from nano-pumice pores. The results of the analysis of the BET nano-pumice selected in this study differ with the various studies that can be attributed to the geological composition of the various sources of this adsorbent. The adsorbent pore diameter has decreased after modification, which can be likely due to

the outer surface of nano-pumice coated with the cationic surfactant.

#### 3.1.6. FTIR analysis

Infrared spectroscopy is based on the adsorption and radiation of the vibrational mutations of molecules and multi-atomic ions. This method is used as a powerful method developed for determining the structure and measuring chemical species. Fig. 4 shows results of FTIR carried out on the nano-pumice adsorbent before and after modification. In the case of the nano-pumice adsorbent, the peak at the wavelength of 3,448.63 1/cm can be attributed to the stretching vibration of the water molecules (humidity) in the –OH and lattice groups (arrangement of atoms in the crystal). The peak appeared at the wavelength of 1,635.3 1/cm belongs to the stretching vibration of OH groups in the water absorbed from the surrounding environment. The peak at the wavelength of 1,022.3 1/cm is related to the stretching vibration bands produced by Si–O and Al–O, the bending mode of which groups formed at wavelengths of 400–500. Additionally, the Si–O–Al stretching vibration is observed at the wavelength of 780.073 1/cm [23]. Generally, the FTIR analysis revealed that pre- and post-modification visible peaks are at nearly the same wavelengths, indicating that the nano-pumice retains its structure after modification.

#### 3.2. Analysis of observations using the surface response curves method and model validation

Table 3 shows the results of CCD-based designing Cr(VI) removal test to develop the mathematical equation.

The adequacy testing of the fitted model was also examined through the distribution plots of the residuals. Fig. 5a shows the distribution of the residuals on the right line in percentage. As shown, the residuals are located on or near the line, and the percentage of the residuals increases as approaching the center of the line. This type of dispersion indicates the normal distribution of the residuals. Fig. 5b shows the amount of residuals against the predicted values. As can be seen, almost half of the residuals are located above the line and the other half at the bottom of the line. This distribution shows that the mean of these values is close to zero,

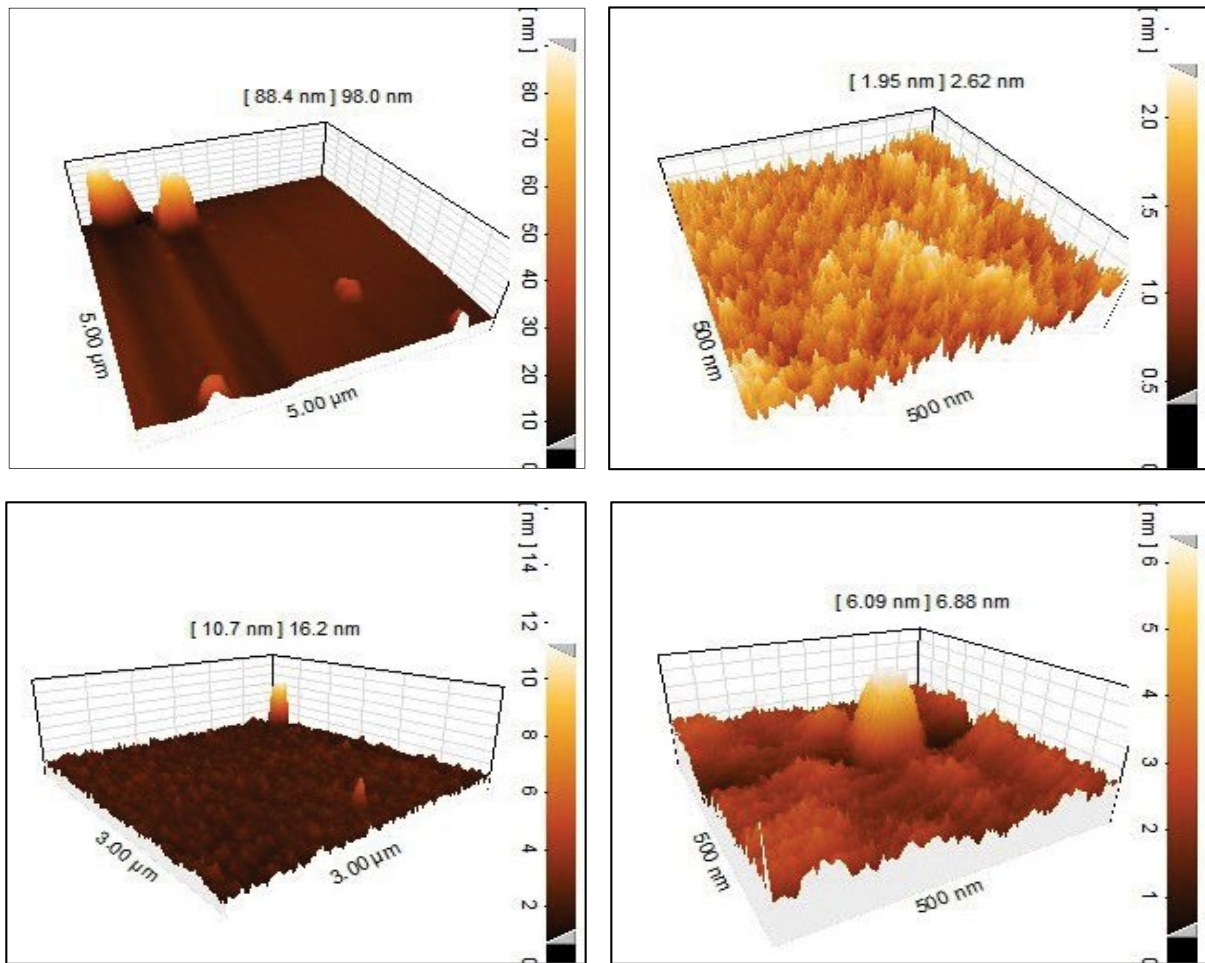


Fig. 3. AFM images of nano-pumice.

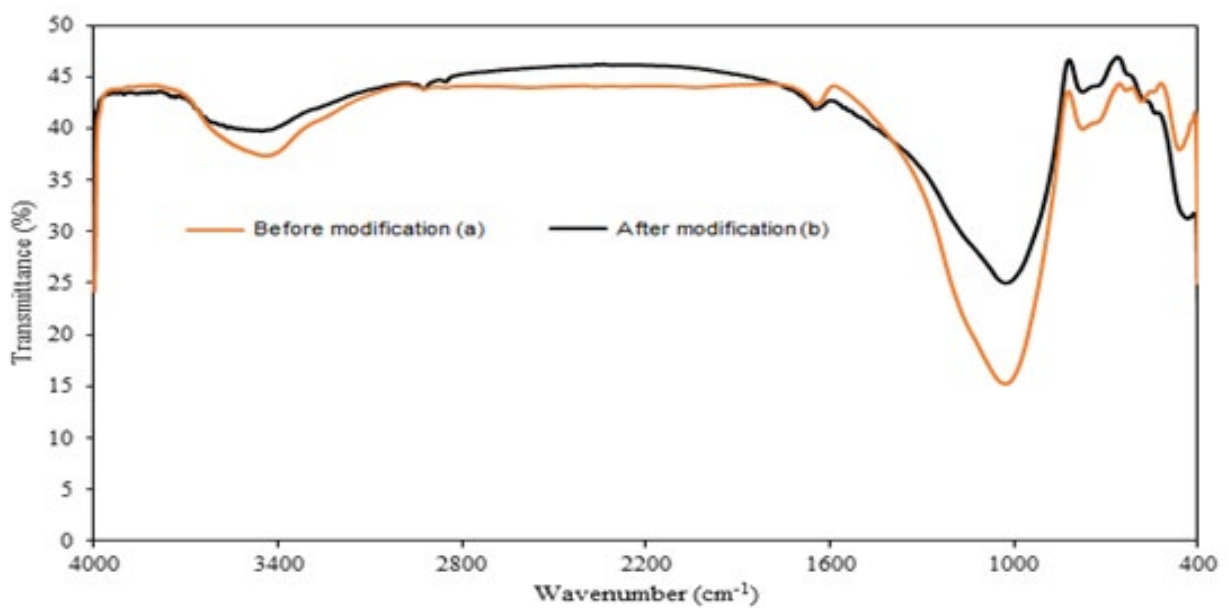


Fig. 4. FTIR spectra of the nano-pumice (a) and pumice/HDTM.Br nano composite (b).

Table 3  
CCD designing chromium (VI) removal by pumice/HDTM.Br nanocomposite

Run	pH	Time (min)	Cr(VI) (mg/L)	Adsorbent dose (g/L)	Y <sub>1</sub>	Y <sub>2</sub>	Run	pH	Time (min)	Cr(VI) (mg/L)	Adsorbent dose (g/L)	Y <sub>1</sub>	Y <sub>2</sub>
1	6	75	0.53	0.55	64	64.99	16	7.5	52.5	0.76	0.78	56	56.60
2	7.5	97.5	0.29	0.33	66	65.43	17	4.5	97.5	0.76	0.33	62	62.81
3	4.5	52.5	0.29	0.78	70	69.24	18	4.5	52.5	0.76	0.33	51	51.22
4	4.5	52.5	0.29	0.33	60	60.34	19	6	75	0.53	0.55	65	64.99
5	4.5	97.5	0.76	0.78	76	76.19	20	7.5	97.5	0.76	0.33	58	57.81
6	7.5	52.5	0.76	0.33	46	46.22	21	6	75	0.53	0.55	65	64.99
7	7.5	97.5	0.29	0.78	78	77.33	22	6	75	0.53	0.55	67	64.99
8	7.5	52.5	0.29	0.33	56	55.34	23	6	75	0.05	0.55	75	75.69
9	4.5	52.5	0.76	0.78	62	61.60	24	6	120	0.53	0.55	74	73.79
10	7.5	97.5	0.76	0.78	71	71.19	25	6	75	0.53	1.00	73	73.19
11	6	75	0.53	0.55	65	64.99	26	6	30	0.53	0.55	49	49.14
12	4.5	97.5	0.29	0.78	82	82.33	27	6	75	0.53	0.10	51	50.75
13	6	75	0.53	0.55	65	64.99	28	3	75	0.53	0.55	70	69.99
14	7.5	52.5	0.29	0.78	64	64.24	29	9	75	0.53	0.55	59	59.99
15	4.5	97.5	0.29	0.33	70	70.43	30	6	75	1.00	0.55	61	60.24

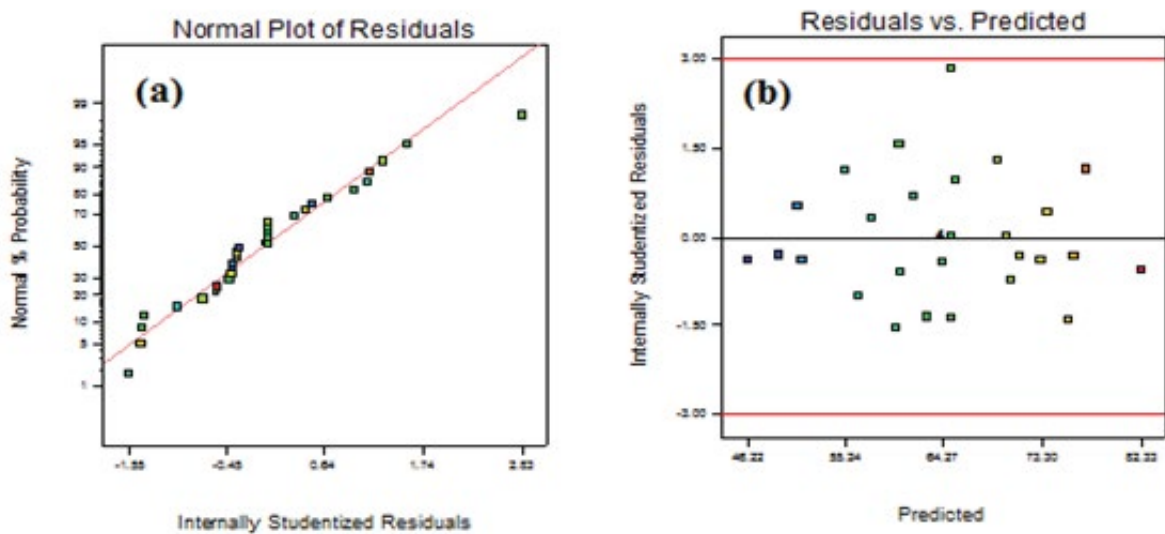


Fig. 5. Conformational analysis of the fitted model for chromium (VI) adsorption.

and changes in residuals do not follow a particular trend and confirm the adequacy of the model [24].

According to the RSM, FO, TWI or SO functions (first-order, first-order interaction and second-order models) are used to determine the regression equations. Multiple R<sup>2</sup> and adjusted R<sup>2</sup> coefficients are the criteria for determining the appropriateness of the polynomial model. Analysis of variance (ANOVA) is also used to match the model and to determine its significance by considering the value of lack of fit test. The criterion for choosing the appropriate model for data matching is the lack of fit ( $p > 0.05$ ). Regardless of the limitations for the model order, the best response surface model (RSM) for the adsorbent was selected as follows. Since the lack of fit test showed a significant first-order model, this model is not a suitable model for data matching. Therefore,

after matching the data with a quadratic model in this study, the quadratic model was used to predict the response variable. The results of regression analysis and ANOVA derived from the quadratic model matching on the Cr(VI) removal by pumice/HDTM.Br nano composite are presented in Tables 4 and 5. The final equation is based on the actual values of various factors as follows:

$$Y (\%) = 64.98 - 5X_1 + 12.31X_2 - 7.67X_3 + 11.21X_4 + 2.99X_2X_4 - 3.52X_2^2 + 2.89X_3^2 - 3.02X_4^2 \quad (5)$$

As can be seen in Table 4, the significant effect is found for first order of all the variables, interaction of time and adsorbent dose and second order of time, Cr(VI) concentration, and adsorbent dose variables on removal

Table 4

Results of regression analysis from the matching of the second-order models on the removal of Cr(VI) by pumice/HDTM.Br nano composite

	Estimate	Std	t value	Pr (> t )
Intercept	64.98	0.30	220.87	2.2e-16***<
pH	-5.00	0.35	-14.34	2.544e-12***
Time	12.31	0.35	35.30	2.2e-16***<
Initial concentration	-7.65	0.35	-21.78	6.722e-16***
Adsorbent dose	11.21	0.35	32.14	2.2e-16***<
Time: Adsorbent dose	2.99	0.85	3.50	0.002**
Time <sup>2</sup>	-3.52	0.65	-5.45	2.047e-05***
Initial concentration <sup>2</sup>	2.89	0.65	4.47	0.0002***
Adsorbent dose <sup>2</sup>	-3.02	0.65	-4.67	0.0001***

Table 5

Results of the analysis of variance obtained from the conformance of the second-order model to the removal of Cr(VI) by pumice/HDTM.Br nano composite

	Df	Sum Sq	Mean Sq	F value	Pr (> F)
FO ( $X_1, X_2, X_3, X_4$ )	4	2,163.40	540.85	741.75	<2.2e-16
TWI ( $X_1, X_4$ )	1	9.00	8.98	12.3	0.002
PQ ( $X_2, X_3, X_4$ )	3	57.30	19.10	26.18	2.724e-07
Residuals	21	15.31	0.73	–	–
Lack of fit	16	10.50	0.65	0.68	0.75
Multiple R-squared	0.99			Adjusted R Squared	0.99

efficiency as the response variable. Considering the ANOVA, the model adequacy is quite clear with regard to the  $p$ -value in the lack of fit test, which is 0.75. According to the adjusted  $R$  squared value, which is equal to the extreme value of 0.99, it can be argued that 99.06 of the adsorption efficiency changes are described according to the variables presented in the proposed model. In other words, the removal of Cr(VI) by the pumice/HDTM.Br nano composite is well defined by the selected second-order model. Therefore, the insignificance of the lack of fit test and the  $R^2$  values indicate the adequacy of the model for the actual values of responses.

### 3.3. Effect of different factors on the chromium (VI) removal efficiency

To achieve a better understanding of the relationship between different parameters and response rates, as well as explain the individual effects and interaction of variables, two-dimensional (2D) plots can be considered, taking into account the performance of two factors and keeping the rest of the factors in the central point. Below, 2-D (Fig. 6) and 3-D (Fig. 7) plots show the efficiency of Cr(VI) removal by the pumice/HDTM.Br nanocomposite.

### 3.4. Investigation of the effect of pH on the Cr(VI) removal efficiency

Based on the values obtained in the regression model (Table 4), the pH coefficient is negative. Considering this

coefficient and what can be seen in the 2-D (Figs. 6a and b) and 3-D (Figs. 7a and b) views of the Cr(VI) removal efficiency decrease as pH of the solution increases from 3 to 9. This phenomenon can be attributed to the change in the surface charge of the pumice/HDTM.Br nano composite. The solution pH has a significant effect on the adsorption process, taking into account pH at the zero charge point of the adsorbent. In other words, if the solution pH is less than  $pH_{pzc}$  of the pumice/HDTM.Br nano composite, then Cr(VI) anions will be adsorbed to a positively charged surface of the adsorbent. At solution pH higher than  $pH_{pzc}$ , adsorptions of Cr(VI) anions occur at very low rate due to the negative charge of pumice/HDTM.Br nanocomposite. The  $pH_{pzc}$  value of 6.3 was obtained for pumice composite/HDTM.Br nano composite. As a result, the pumice/HDTM.Br nano composite surface is negatively charged in aqueous solutions with pH higher than  $pH_{pzc}$  and Cr(VI) ion is eliminated by this adsorbent, which results in the reduction of the removal efficiency. In addition, the fact that adsorption of Cr(VI) was reduced in case of increasing pH levels can be due to the increase in the formation of  $-OH$  ions, and the competitive adsorption of Cr(VI) onto the available adsorption sites. The adsorption of Cr(VI) ions will be higher on the positively charged surface of the adsorbent in solutions with pH less than 6.3, which is due to the electrostatic attraction between soluble ions and the positive charge of the adsorbent surface. Another study reports that the removal efficiency will be reduced with increasing pH values [25].

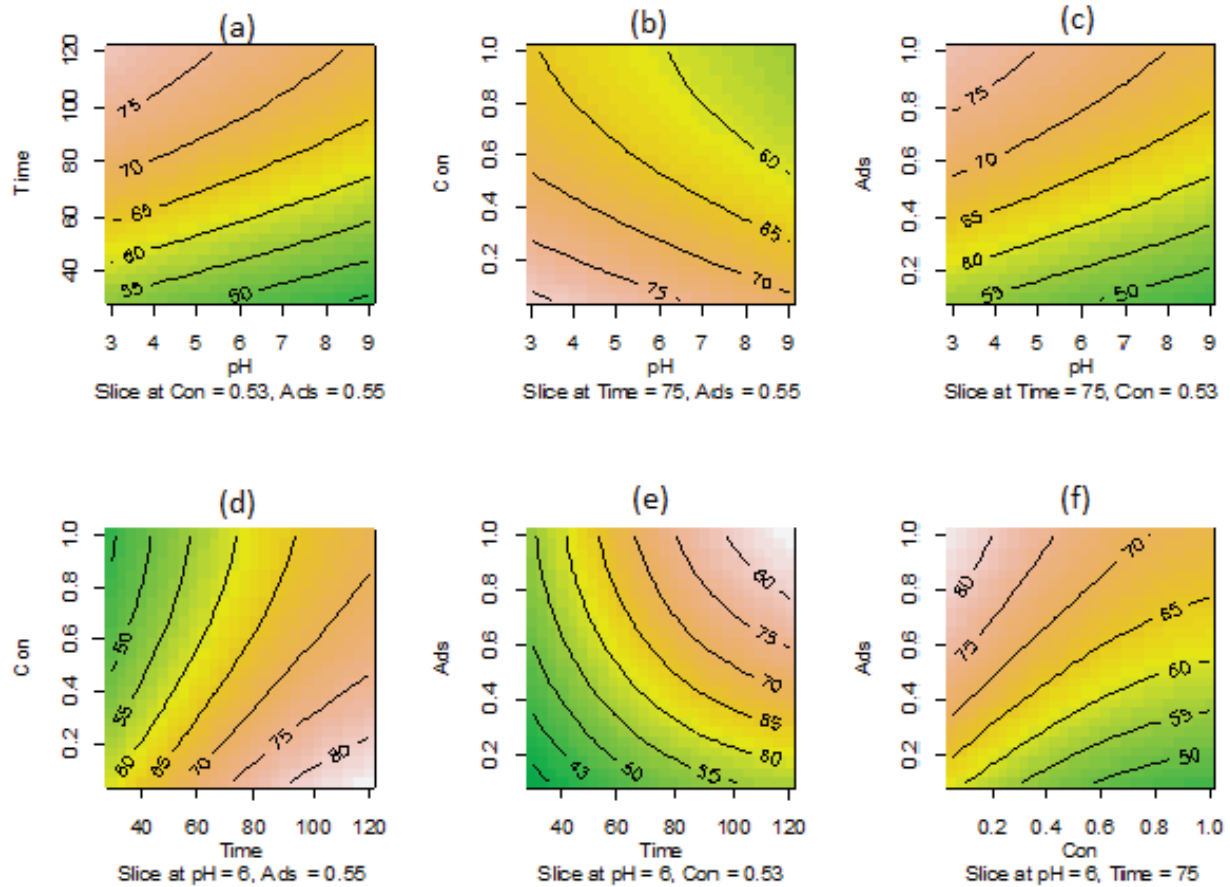


Fig. 6. The 2D plots of combined effect of pH, adsorbent dosage (g/L), Cr(VI) concentration (mg/L) and time (min) on removal efficiency of Cr(VI) using pumice absorbent/HDTM.Br nanocomposite.

### 3.5. Investigation of the effect of chromium (VI) initial concentration on the Cr(VI) removal efficiency

The initial concentration of the contaminants is one of the factors that affect the adsorption process. Regarding the negative values of the initial concentration coefficients of Cr(VI) in the regression model (Table 4) as well as the contour plots (Figs. 6d and f) and 3-D plots (Figs. 7e and f), it can be concluded that the Cr(VI) removal efficiency is reduced as the concentration of Cr(VI) in the solution increases from 0.05 to 1 mg/L. In fact, with increasing concentrations of the contaminant, the ratio of the available adsorbent to contaminant concentration is reduced, and the adsorbent surface has limited and specific points for the contaminant. Therefore, the further removal of Cr(VI) at lower concentrations is due to the availability of free adsorption sites at low concentrations of the adsorbent material [26]. Differences between the results of this study and those of other studies are probably due to differences in the Cr(VI) concentrations.

### 3.6. Investigation of the effect of adsorbent dose on the removal efficiency of Cr(VI)

Determining the effect of adsorbent dose, due to its impact on the economy of the adsorption process for

designing large commercial-industrial systems, is one of the most important issues in these systems [27]. As the results show, based on regression model coefficients in Eq. (5), the adsorbent dose with high regression coefficient has a potential effect on the removal of Cr(VI) from aqueous solutions. According to (Figs. 6e and c) and (Figs. 7d and c), the removal efficiency increases as the adsorbent dose increases from 0.1 to 1 g/L. This process happens due to increasing active and effective surface areas during the adsorption process. Since the efficiency depends on different factors, the appropriate dose for Cr(VI) removal test is 1 g. Although increasing adsorbent concentrations lead to an increase in the removal efficiency of contaminants, because of the lower concentration of the contaminant, the amount of adsorption per unit mass of adsorbent is reduced [28]. The results of this study show that elevated adsorbent amounts have a significant effect on the efficiency of chromate removal. These results are also consistent with studies carried out by other researchers [29].

### 3.7. Investigating the effect of contact time on removal of chromium (VI)

In general, the contact time is an effective factor in discontinuous systems. However, these conditions can vary

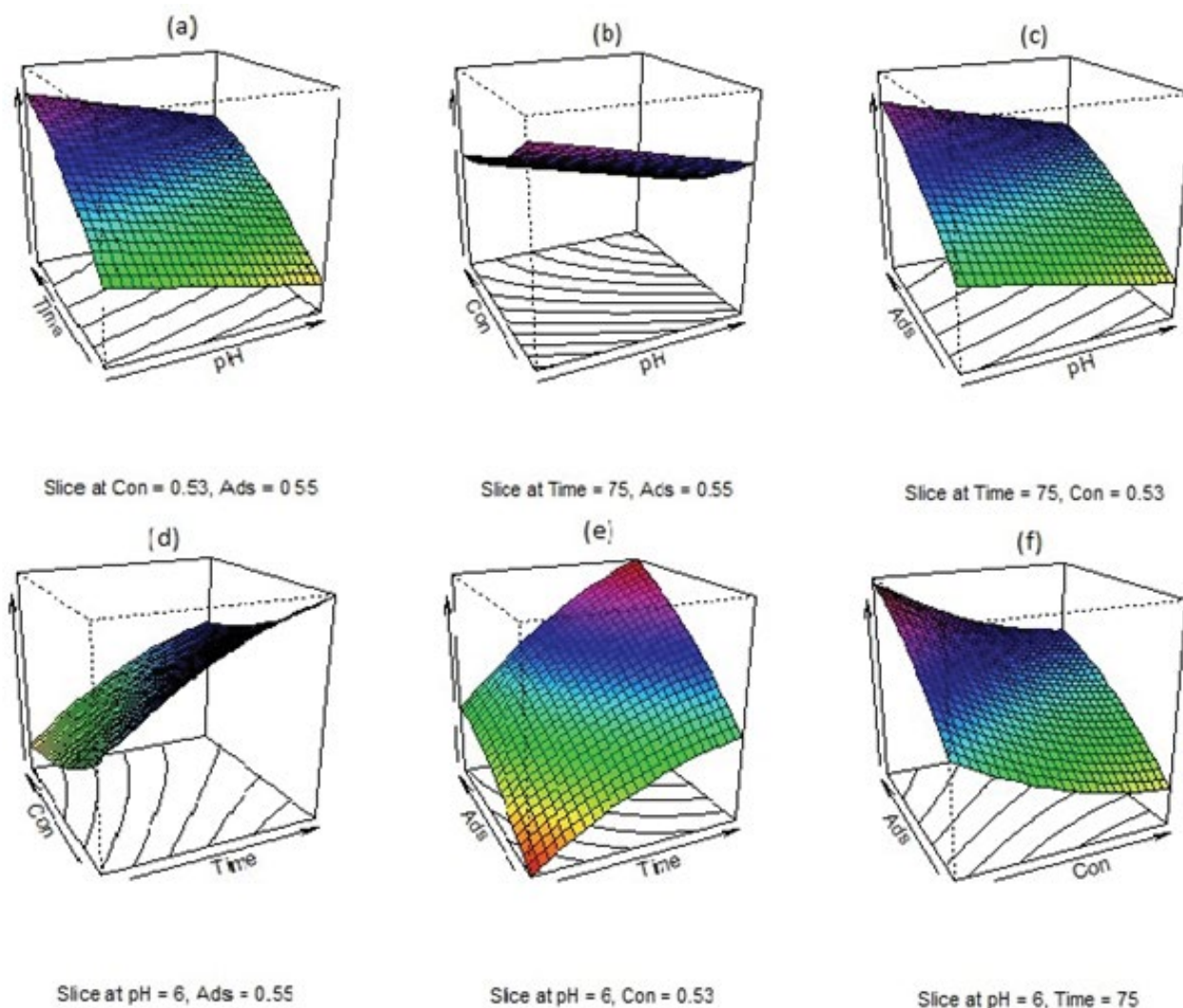


Fig. 7. The 3D plots of combined effect of pH, adsorbent dosage (g/L), Cr(VI) concentration (mg/L) and time (min) on removal efficiency of Cr(VI) using pumice adsorbent/HDTM.Br nanocomposite.

depending on the characteristics of the initial solution and the type of adsorbent. In the present study, based on a discontinuous system, samples were examined at time intervals of 30–120 min. Regarding the positive coefficients of the regression model as well as the 2-D and 3-D plots presented in Figs. 6d and e and Figs. 7d and e, it can be concluded that this parameter has an incremental effect on the removal of the Cr(VI) contaminant from the solution. As can be seen, the removal efficiency of Cr(VI) increases as adsorbent contact time as well as the amount of adsorbent increases. The results of this study were consistent with other previous studies on adsorption [30].

### 3.8. Investigating the optimal values for each of the variables

The results of optimizing the parameters using cross-numerical methods showed that the maximum removal efficiency of Cr(VI) by pumice/HDTM.Br nano composite adsorbent was equal to 96.22% at pH = 3 (less than  $pH_{pzc}$

value). To achieve the maximum removal efficiency, the amount of 1 g/L of 0.05 mg/L of the initial concentration of Cr(VI) and contact time of 120 min are required.

### 3.9. Adsorption kinetic study

For the purpose studying the velocity constant of adsorption processes, pseudo-first order, pseudo-second order kinetic models and particle diffusion were used. The kinetic study was performed according to optimal conditions of initial concentration of 0.05 mg/L, contact time of 120 min, adsorbent dose of 1 g/L and pH = 3. The equations of pseudo-first order, pseudo-second-order kinetic models and intraparticle diffusion are presented below, respectively:

$$\ln(q_e - q_t) = \ln q_e - k_1 t \quad (6)$$

$$\frac{t}{q_t} = \frac{1}{k_2 q_e^2} + \left( \frac{t}{q_e} \right) \tag{7}$$

$$q_t = k_i t^{0.5} + C \tag{8}$$

In these equations,  $q_t$  (mg/g) is the adsorption capacity at equilibrium time (min),  $k_1$  is reaction constant of pseudo-first-order reaction mg/g min,  $k_2$  is reaction rate constant of pseudo-second-order reaction mg/g min,  $q_e$  is the amount of adsorption capacity on the adsorbent in the equilibrium state (mg/g),  $k_i$  is the intraparticle diffusion kinetic (mg of adsorbate per g of adsorbent per min (mg/g min<sup>0.5</sup>)) and (mg/g),  $C$  is the adsorption constant. The values of the pseudo-first-order kinetic model are obtained by plotting the linear plot of  $\ln(q_e - q_t)$  against  $t$  in such way that  $k_1$  and  $q_e$  are obtained from the line gradient and the result of 2.71 to the power of y-intercept. The values of the pseudo-second-order kinetic model are obtained by plotting the linear plot of  $t/q_t$  against  $t$  in such way that line gradient and y-intercept values are equal to  $1/q_e$  and  $1/k_2 q_e^2$ , respectively. Also, the values of the intraparticle diffusion model are obtained by plotting the linear plot of  $q_t$  against  $t^{1.2}$ . Table 6 shows the parameters obtained from the analysis of the data obtained from the Cr(VI) adsorption process on the pumice/HDTM.Br nano composite adsorbent. According to this table, these correlation coefficients ( $R^2$ ) and the closeness of the experimental and computational adsorption capacity values of  $q_e$  (exp) (mg/g) show that the Cr(VI) adsorption is highly compatible with the pseudo-second order model. According to the foregoing, it can be concluded that the rate of Cr(VI) adsorption on pumice/HDTM.Br nanoparticle adsorbent depends on the nature of both adsorbent and adsorbate agents, hence it can be said that the adsorption is of chemical type. Considering the unique physical properties, porosities and vacancies of the pumice/HDTM.Br nano composite adsorbent, it can be argued that a factor such as intraparticle diffusion is an effective factor in controlling the adsorption rate. Table 6 shows values calculated for intraparticle diffusion equation parameters. Considering the correlation coefficients calculated in this table, it can be concluded that Cr(VI) adsorption on the pumice/HDTM.Br nano composite adsorbent ( $R^2 = 0.96$ ) is highly compatible with this model. The results of our study are consistent

with some studies on the adsorption of Cr(VI) on various adsorbents [31].

### 3.10. Adsorption isotherm study

Isotherm equations show the relationship between adsorbate concentration on adsorbent surface in vitro and its equilibrium concentration in the liquid phase. Thus, by examining the adsorption isotherms, it is possible to determine the maximum adsorption capacity and define an equation with the aim of designing the adsorption column [32]. Therefore, after determining the optimal values of time, pH, initial concentration of Cr(VI) and adsorbent dose, characteristics of Cr(VI) adsorption isotherm on pumice/HDTM.Br nano composite were determined. Empirical data on adsorption equilibrium were analyzed using Langmuir, Freundlich and Temkin isotherm studies. Freundlich isotherm is an empirical formula based on adsorption on a heterogeneous surface. The linear form of the Freundlich isotherm model is expressed as follows:

$$q_e = K_f C_e^{\frac{1}{n}} \tag{9}$$

In Freundlich equation,  $q_e$  represents the number of metal ion adsorbents per unit mass of the adsorbent (mg/g),  $C_e$  represents the equilibrium concentration of metal ions (mg/L),  $K_f$  (l/g) and  $1/n$  are Freundlich constants that show the adsorption capacity and intensity, respectively. The value of  $n$  is an indicator for the isotherm desirability, where the  $n$  values 2–10, 1–2 and less than 1 shows desirability, relative desirability, and weakness of the adsorption profile, respectively [33]. According to Table 7, the correlation coefficient of the Freundlich model with the highest  $R^2$  value ( $R^2 > 0.99$ ) has the highest compliance with experimental data. Accordingly, the type of adsorption process can be described as adsorption of Cr(VI) in layers, in which Cr(VI) initially reacts with the adsorbent column and subsequently with each other, occurs on a heterogeneous surface in terms of energy. These findings are consistent with the findings from other studies [34]. The  $n$  value, as a constant value, was reported to be between 1 and 2 in the Freundlich model, which indicates the relative desirability of Cr(VI) adsorption on the pumice/HDTM.Br nano composite adsorbent in vitro.

Table 6  
Results of the adsorption kinetic study of chromium (VI) on the pumice/HDTM.Br nano composite adsorbent

Adsorbent	Pseudo-first-order			Pseudo-second-order			Intraparticle diffusion		
	$q_e$ (exp) (mg/g)	$k_1$	$R^2$	$q_e$ (exp)(mg/g)	$k_2$	$R^2$	$C$ (mg/g)	$k_i$	$R^2$
Pumice/HDTM.Br nano composite	0.0083	0.03	0.98	0.012	3.75	0.99	0.001	0.005	0.96

Table 7  
Results of the adsorption isotherm study of chromium (VI) on the pumice/HDTM.Br nano composite adsorbent

Adsorbent	Freundlich			Langmuir				Temkin		
	$K_f$	$n$	$R^2$	$q_e$ (mg/g)	$b$	$R_L$	$R^2$	$k_T$	$B_T$	$R^2$
Pumice/HDTM.Br nano composite	0.64	1.5	0.99	0.24	15.46	0.06–0.56	0.80	552	0.033	0.82

Table 8  
Relationship between  $R_L$  parameter and Cr(VI) adsorption on the pumice/HDTM.Br nano composite adsorbent

$R_L$ values	Isotherm situation
$R_L > 1$	Unfavorable
$R_L = 1$	Linear
$R_L = 0$	Irreversible
$0 < R_L < 1$	Favorable

Langmuir isotherm model suggests a single-layer adsorption on a homogeneous surface of the adsorbent without inducing any reaction between adsorbent molecules with uniform adsorption energy [35]. Langmuir isotherm model equation is as follows:

$$C_e \frac{1}{q_m} + \frac{C_e}{q_m} = \frac{q_e}{q_{mb}} \quad (10)$$

where  $q_m$  represents the maximum adsorption capacity (mg/g),  $C_e$  represents the contaminant equilibrium concentration (mg/L),  $q_e$  represents the amount of contaminant per unit mass of the adsorbent (mg/g), and  $b$  is Langmuir constant (l/mg).

One of the features of the Langmuir equation is the dimensionless parameter of the isolation coefficient of  $R_L$ , which is calculated from Eq. (11):

$$R_L = \frac{1}{(1 + bC_0)} \quad (11)$$

$C_0$  is the initial concentration of Cr(VI) (mg/L). The type of adsorption process can be determined using this parameter. The values proposed for this parameter are shown in Table 8 [36].

According to Table 8, the  $R_L$  values of the Langmuir isotherm ranges between 0 and 1, indicating that the isotherm is desirable. Based on this isotherm model, the maximum adsorption capacity ( $q_m$ ) for pumice/HDTM.Br nano composite adsorbent is equal to 0.24 mg/g, the trend of which is consistent with the BET results indicating an increase in the SSA values (9.79 m<sup>2</sup>/g). Temkin isotherm model shows the effects of indirect reactions between adsorbent and adsorbate on adsorption isotherm. The Temkin isotherm model equation is presented below:

$$B_T \ln k_T + B_T \ln C_e = q_e \quad (12)$$

where  $R$  is the gas constant (kJ mol/K),  $T$  is temperature (K),  $B_T = (RT)/b$  is Temkin constant, and  $k_T$  (L/g) is a force constant and a criterion for the maximum energy of the bond. The high  $B_T$  value indicates that the adsorption of metal ions is faster in the first stage. According to the  $B_T$  value of 0.0334 (Table 7), it can be argued that the high adsorption of Cr(VI) anions on the nano pumice /HDTM.Br composite adsorbent does not occur in the first stage. Similarly, the high value of  $k_T$  represents a strong adsorbate–adsorbent binding. Thus, with respect to the  $k_T$  value of 552 (Table 7), it can be argued that

there is a strong bond between the Cr(VI) ions and the surfaces of nano pumice/HDTM.Br composite particles.

Comparing the maximum adsorption capacities of Cr(VI) ions among various adsorbents, the nano pumice/HDTM.Br composite adsorbent used in this study exhibited a much higher adsorption capacity than the other reported adsorbents, for example, 0.2 and 0.15 mg/g by clay (treated), and riverbed sand, respectively [37,38].

#### 4. Conclusion

In this study, nano pumice/HDTM.Br composite was tested for the removal of Cr(VI) from aqueous solutions. It was also a function of initial concentration, contact time, pH, sorbents dose and co-existing anion of the solution. The maximum adsorption capacity of Cr(VI) at equilibrium was 0.24 mg/g at a dose of 1 g/L with initial Cr(VI) concentration of 0.05 mg/L at optimum pH of 3. The kinetic study showed that the pseudo-second order model is suitable for describing the experimental data. The adsorption can be well described by Freundlich isotherm model. Therefore, removal of Cr(VI) from aqueous solutions by adsorption onto pumice/HDTM.Br nano composite as alternative low-cost adsorbent appears to be feasible given high removal efficiency (about 96%). Further studies have to be done using real samples from industrial effluents.

#### Acknowledgment

The authors would like to thank Deputy of Research, Tehran University of Medical Sciences for their financial support for this research as Grant # 36506.

#### References

- [1] M. Ghanbarian, R. Nabizadeh, S. Nasser, F. Shemirani, A.H. Mahvi, M.H. Beyki, A. Mesdaghinia, Potential of amino-riched nano-structured MnFe<sub>2</sub>O<sub>4</sub>@ cellulose for biosorption of toxic Cr (VI): modeling, kinetic, equilibrium and comparing studies, *Int. J. Biol. Macromol.*, 104 (2017) 465–480.
- [2] M. Mirzabeygi, A. Abbasnia, M. Yunesian, R.N. Nodehi, N. Yousefi, M. Hadi, A.H. Mahvi, Heavy metal contamination and health risk assessment in drinking water of Sistan and Baluchistan, Southeastern Iran, *Human Ecol. Risk Assess.* *Int. J.*, 23 (2017) 1893–1905.
- [3] E. Bazrafshan, A.H. Mahvi, S. Naseri, A.R. Mesdaghinia, Performance evaluation of electrocoagulation process for removal of chromium (VI) from synthetic chromium solutions using iron and aluminum electrodes, *Turkish J. Eng. Environ. Sci.*, 32 (2008) 59–66.
- [4] A. Mahvi, F. Gholami, S. Nazmara, Cadmium biosorption from wastewater by Ulmus leaves and their ash, *Eur. J. Sci. Res.*, 23 (2008) 197–203.
- [5] A. Asgari, F. Vaezi, S. Nasser, O. Dördelmann, A. Mahvi, E.D. Fard, Removal of hexavalent chromium from drinking water by granular ferric hydroxide, *J. Environ. Health Sci. Eng.*, 5 (2008) 277–282.
- [6] E. Bazrafshan, L. Mohammadi, A. Ansari-Moghaddam, A.H. Mahvi, Heavy metals removal from aqueous environments by electrocoagulation process—a systematic review, *J. Environ. Health Sci. Eng.*, 13 (2015) 74.
- [7] H.J. Mansoorian, A.H. Mahvi, A.J. Jafari, Removal of lead and zinc from battery industry wastewater using electrocoagulation process: influence of direct and alternating current by using iron and stainless steel rod electrodes, *Sep. Purif. Technol.*, 135 (2014) 165–175.

- [8] R. Klimaviciute, J. Bendoraitiene, R. Rutkaite, A. Zemaitaitis, Adsorption of hexavalent chromium on cationic cross-linked starches of different botanic origins, *J. Hazard. Mater.*, 181 (2010) 624–632.
- [9] A. Maleki, A.H. Mahvi, M.A. Zazouli, H. Izanloo, A.H. Barati, Aqueous cadmium removal by adsorption on barley hull and barley hull ash, *Asian J. Chem.*, 23 (2011) 1373.
- [10] R. Khosravi, M. Fazlzadehdavil, B. Barikbin, A.A. Taghizadeh, Removal of hexavalent chromium from aqueous solution by granular and powdered *Peganum Harmala*, *Appl. Surface Sci.*, 292 (2014) 670–677.
- [11] G.H. Safari, M. Zarrabi, M. Hoseini, H. Kamani, J. Jaafari, A.H. Mahvi, Trends of natural and acid-engineered pumice onto phosphorus ions in aquatic environment: adsorbent preparation, characterization, and kinetic and equilibrium modeling, *Desal. Wat. Treat.*, 54 (2015) 3031–3043.
- [12] T. Liu, Z.-L. Wang, X. Yan, B. Zhang, Removal of mercury (II) and chromium (VI) from wastewater using a new and effective composite: pumice-supported nanoscale zero-valent iron, *Chem. Eng. J.*, 245 (2014) 34–40.
- [13] S.H. Khorzughy, T. Eslamkish, F.D. Ardejani, M.R. Heydartaemeh, Cadmium removal from aqueous solutions by pumice and nano-pumice, *Korean J. Chem. Eng.*, 32 (2015) 88–96.
- [14] Z. Derakhshan, M.H. Ehrampoush, A.H. Mahvi, M. Faramarzi, M. Mokhtari, S.M. Mazloomi, Evaluation of volcanic pumice stone as media in fixed bed sequence batch reactor for atrazine removal from aquatic environments, *Water Sci. Technol.*, 74 (2016) 2569–2581.
- [15] M.N. Sepehr, A. Amrane, K.A. Karimaian, M. Zarrabi, H.R. Ghaffari, Potential of waste pumice and surface modified pumice for hexavalent chromium removal: characterization, equilibrium, thermodynamic and kinetic study, *J. Taiwan Inst. Chem. Eng.*, 45 (2014) 635–647.
- [16] T. Liu, Y. Yang, Z.-L. Wang, Y. Sun, Remediation of arsenic (III) from aqueous solutions using improved nanoscale zero-valent iron on pumice, *Chem. Eng. J.*, 288 (2016) 739–744.
- [17] A.H. Mahvi, B. Heibati, A. Mesdaghinia, A.R. Yari, Fluoride adsorption by pumice from aqueous solutions, *J. Chem.*, 9 (2012) 1843–1853.
- [18] A.H. Mahvi, B. Heibati, Removal of Reactive Red 120 and Direct Red 81 dyes from aqueous solutions by pumice, *Res. J. Chem. Environ.*, 16 (2012) 62–68.
- [19] T. sahan, D. Ozturk, Investigation of Pb (II) adsorption onto pumice samples: application of optimization method based on fractional factorial design and response surface methodology, *Clean Technol. Environ. Policy*, 16 (2014) 819–831.
- [20] H. Shayesteh, A. Rahbar-Kelishami, R. Norouzbeigi, Evaluation of natural and cationic surfactant modified pumice for congo red removal in batch mode: kinetic, equilibrium, and thermodynamic studies, *J. Mol. Liq.*, 221 (2016) 1–11.
- [21] M.R. Samarghandi, M. Zarrabi, A. Amrane, M.M. Soori, M.N. Sepehr, Removal of acid black dye by pumice stone as a low cost adsorbent: kinetic, thermodynamic and equilibrium studies, *Environ. Eng. Manage. J.*, 12 (2013) 2137–2147.
- [22] S. Habibi, A. Nematollahzadeh, S.A. Mousavi, Nano-scale modification of polysulfone membrane matrix and the surface for the separation of chromium ions from water, *Chem. Eng. J.*, 267 (2015) 306–316.
- [23] M.N. Sepehr, V. Sivasankar, M. Zarrabi, M.S. Kumar, Surface modification of pumice enhancing its fluoride adsorption capacity: an insight into kinetic and thermodynamic studies, *Chem. Eng. J.*, 228 (2013) 192–204.
- [24] S. Sugashini, K.M.S. Begum, Optimization using central composite design (CCD) for the biosorption of Cr (VI) ions by cross linked chitosan carbonized rice husk (CCACR), *Clean Technol. Environ. Policy*, 15 (2013) 293–302.
- [25] V. Srivastava, Y. Sharma, M. Sillanpaa, Response surface methodological approach for the optimization of adsorption process in the removal of Cr (VI) ions by  $\text{Cu}_2(\text{OH})_2\text{CO}_3$  nanoparticles, *Appl. Surface Sci.*, 326 (2015) 257–270.
- [26] T. Liu, Z.-L. Wang, Y. Sun, Manipulating the morphology of nanoscale zero-valent iron on pumice for removal of heavy metals from wastewater, *Chem. Eng. J.*, 263 (2015) 55–61.
- [27] G. Asgari, A. Ebrahimi, A.S. Mohammadi, G. Ghanizadeh, The investigation of humic acid adsorption from aqueous solutions onto modified pumice with hexadecyl trimethyl ammonium bromide, *Int. J. Environ. Health Eng.*, 2 (2013) 20.
- [28] A.M. Yusof, N.A.N.N. Malek, Removal of Cr (VI) and As (V) from aqueous solutions by HDTMA-modified zeolite Y, *J. Hazard. Mater.*, 162 (2009) 1019–1024.
- [29] M. Noroozifar, M. Khorasani-Motlagh, M. Gorgij, H. Naderpour, Adsorption behavior of Cr (VI) on modified natural zeolite by a new bolaform N, N, N, N', N', N'-hexamethyl-1, 9-nonanediammonium dibromide reagent, *J. Hazard. Mater.*, 155 (2008) 566–571.
- [30] K. Anupam, S. Dutta, C. Bhattacharjee, S. Datta, Adsorptive removal of chromium (VI) from aqueous solution over powdered activated carbon: optimisation through response surface methodology, *Chem. Eng. J.*, 173 (2011) 135–143.
- [31] D. Gusain, F. Bux, Y.C. Sharma, Abatement of chromium by adsorption on nanocrystalline zirconia using response surface methodology, *J. Mol. Liq.*, 197 (2014) 131–141.
- [32] L. Rafati, A. Mahvi, A. Asgari, S. Hosseini, Removal of chromium (VI) from aqueous solutions using Lewatit FO36 nano ion exchange resin, *Int. J. Environ. Sci. Technol.*, 7 (2010) 147–156.
- [33] H. Golestani, B. Haibati, H. Amini, M.H. Dehghani, A. Asadi, Removal of hexavalent chromium from aqueous solution by adsorption on  $\gamma$ -alumina nanoparticles, *Environ. Protect. Eng.*, 41 (2015) 133–145.
- [34] M. Yavuz, F. Gode, E. Pehlivan, S. Ozmert, Y.C. Sharma, An economic removal of  $\text{Cu}^{2+}$  and  $\text{Cr}^{3+}$  on the new adsorbents: pumice and polyacrylonitrile/pumice composite, *Chem. Eng. J.*, 137 (2008) 453–461.
- [35] S. Nasser, M. Heidari, Evaluation and comparison of aluminum-coated pumice and zeolite in arsenic removal from water resources, *Iranian J. Environ. Health Sci. Eng.*, 9 (2012) 38.
- [36] A.G. Yavuz, E. Dincturk-Atalay, A. Uygun, F. Gode, E. Aslan, A comparison study of adsorption of Cr (VI) from aqueous solutions onto alkyl-substituted polyaniline/chitosan composites, *Desalination*, 279 (2011) 325–331.
- [37] T.A. Khan, V.V. Singh, Removal of cadmium (II), lead (II), and chromium (VI) ions from aqueous solution using clay, *Toxicol. Environ. Chem.*, 92 (2010) 1435–1446.
- [38] Y. Sharma, C. Weng, Removal of chromium (VI) from water and wastewater by using riverbed sand: Kinetic and equilibrium studies, *J. Hazard. Mater.*, 142 (2007) 449–454.